The fragmentation of expanding shells: cloud formation rates and masses

Jan Palouš, Richard Wünsch and Soňa Ehlerová

Astronomical Institute, Academy of Sciences of the Czech Republic, Boční II 1401, 141 31 Prague 4, Czech Republic

Abstract. The gravitational instability of expanding shells is discussed. Linear and nonlinear terms are included in an analytical solution in the static and homogeneous medium. We discuss the interaction of modes and give the time needed for fragmentation. Masses of individual fragments are also estimated and their formation rates and the initial mass function are derived. Results of simulations are compared to observation.

1. Introduction

The time evolution of the gravitational collapse of perturbations in decelerating, isothermal shocked layers has been examined numerically and analytically using linearized equations by Elmegreen (1994). In this paper, we continue with nonlinear analysis of the gravitational instability of spherically symmetric shells expanding into the stationary homogeneous medium. We modify the approach adopted by Fuchs (1996) who described the fragmentation of uniformly rotating self-gravitating disks. The inclusion of higher order terms helps to determine with better accuracy when, where and how quickly the fragmentation happens. Formation rates and the mass distribution function of fragments are derived from simulations and compared to the observed mass spectrum of molecular clouds.

2. Hydrodynamical and Poisson equations on the surface of a thin shell

Equations as derived by Wünsch & Palouš (2001) are

$$\frac{\partial m}{\partial t} + (\nabla, m\vec{v}) = A\,V\rho_0, \tag{1}$$

$$\frac{1}{A}\frac{d(m\vec{v})}{dt} = -c^2\nabla\Sigma - \Sigma\nabla\Phi, \tag{2}$$

$$\Delta\Phi = 4\pi G\Sigma\delta(z)\,, \tag{3}$$

where V is the expansion velocity of the shell, m is mass in the area A on the surface of the shell, and $\vec{v}$ denotes a two dimensional velocity of surface flows. Σ is the surface density, c is the constant isothermal sound speed inside the cold
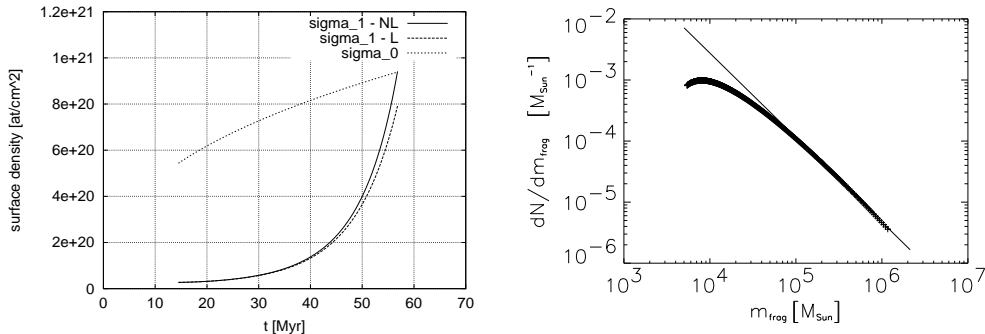
Figure 1.   Left: the evolution of the maximum surface density perturbation in the linear and nonlinear case. Right: the mass spectrum of fragments. The straight line is the power law fit of the decreasing part of the spectrum $m_{frag}^{-1.4}$.

shell, Φ is the gravitational potential generated by the mass distribution in the shell, G is the gravitational constant and $\delta(z)$ is a delta function of the space coordinate z perpendicular to the surface of the shell.

2.1.   The linear solution

The solution of linearized Eq. (1 - 3) may be written in the form of exponential functions for the perturbations: Σ_{1-L} (perturbed surface density) and $\vec{v} \sim e^{i\omega t}$. The shell starts to be gravitationally unstable when

$$\omega = i\frac{3V}{R} - \sqrt{-\frac{V^2}{R^2} + \frac{\eta^2 c^2}{R^2} - \frac{2\pi G \Sigma_0 \eta}{R}} \qquad (4)$$

is purely imaginary and negative. R denotes the radius and Σ_0 the unperturbed surface density of the shell. ω is the angular frequency, in the case of instability $i\omega$ gives the perturbation growth rate, and η the wave number of perturbations. The time evolution of Σ_0 and of Σ_{1-L}, is shown in Fig. 1 for shell expanding in the homogeneous medium of the constant volume density 1 cm^{-3} and average atomic weight 1.3. The total energy released is 10^{53} erg and $c = 1$ km s^{-1}.

2.2.   The nonlinear analysis

Wünsch & Palouš (2001) include quadratic terms into equations for the evolution of perturbations. The time evolution of the perturbed maximum surface density including nonlinear terms, Σ_{1-NL}, is given in Fig. 1. As another result of the nonlinear analysis Fig. 2 shows the spatial distribution of the surface density and velocity vectors of the surface flows resulting from mode interactions.

3.   Time evolution of fragments and their mass spectrum

After the time when the shell becomes unstable, the mass of the fragment decreases as its size decreases. Later, the inflow of mass begins to dominate (surface
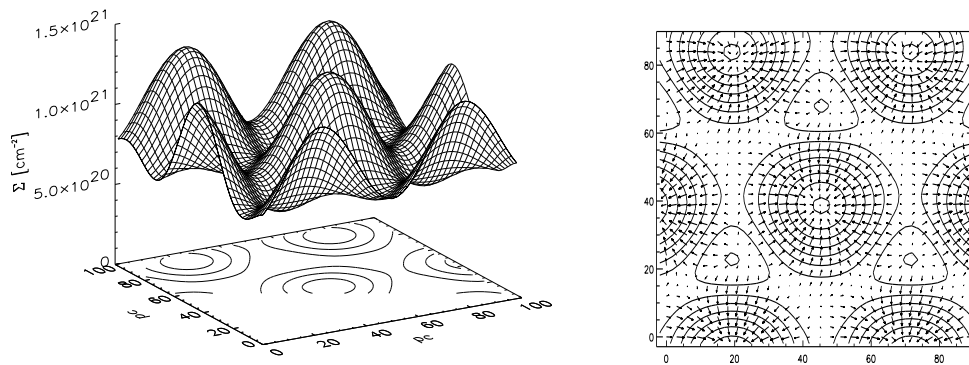
Figure 2.   Left: the spatial distribution of the surface density at $t = 50$ Myr. Right: velocity vectors of the surface flows at the same time.

flows are shown in Fig. 2) and the fragment mass grows. Masses of individual fragments are between a few times $10^3 M_\odot$ and $1.5 \times 10^6 M_\odot$ with the highest frequency around $m_{frag} \sim 10^4 M_\odot$. Another consequence of the dispersion relation (4) is that the most massive fragments, corresponding to the smallest unstable wave number η, form very slowly. Therefore, the most massive clouds are created at the latest stages of the shell evolution. The mass spectrum of fragments is shown in Fig. 1. Its decreasing part can be approximated with a power law $dN/dm_{frag} \sim m_{frag}^\alpha$ where $\alpha = -1.4$. This is quite close to the observed mass spectrum of GMC in the Milky Way. Combes (1991) gives $\alpha = -1.5$. NAN-TEN survey of the CO emission of the LMC (Fukui, 2001) gives steeper slope: $\alpha = -1.9$, which may be connected to higher level of random motions in the LMC compared to the Milky Way, which restricts the formation of late time massive fragments in the LMC and steepens their mass spectrum.

References

Combes F. 1991, ARA&A29, 195

Elmegreen, B. G. 1994, ApJ427, 384

Fuchs, B. 1996, MNRAS287, 985

Fukui Y. 2001, this proceedings

Wünsch R., & Palouš J. 2001, A&A, in press